Geometric magnetic frustration in the hexagonal perovskite $(\text{La},\text{Sr})_{4-z}\text{RuO}_{7+\delta}$

Stefan G. Ebbinghaus,[1,*] Ernst-Wilhelm Scheidt,[2] and Thomas Götzfried[1]

[1]*Lehrstuhl für Festkörperchemie, Institut für Physik, Universität Augsburg, Universitätsstraße 1, D-86159 Augsburg, Germany*
[2]*Chemische Physik und Materialwissenschaften, Institut für Physik, Universität Augsburg, Universitätsstraße 1,*
D-86159 Augsburg, Germany

The hexagonal perovskite $(\text{La},\text{Sr})_{4-z}\text{RuO}_{7+\delta}$ exhibits a strong magnetic frustration due to the geometric arrangement of the paramagnetic Ru^{5+} ions, which form a network of edge-sharing elongated tetrahedra. In this magnetic sublattice, frustration may either be restricted to the crystallographic ab plane, in which the ruthenium ions form a triangle lattice, or concern the entire tetrahedra. Crystals of $(\text{La},\text{Sr})_{4-z}\text{RuO}_{7+\delta}$ were grown by the floating zone method, and their magnetic properties were measured with respect to the crystallographic axes. Magnetic ordering was only detected for the external magnetic field parallel to the ab plane, while for $\mathbf{B}\|c$ the samples showed no magnetic transition down to 2 K. Heat capacity measurements revealed a magnetic entropy corresponding to a spin of 1/2, a value much smaller than the $S=3/2$ expected for the $(t_{2g})^3$ configuration of Ru^{5+} ions. From symmetry considerations, we conclude that only the orbitals corresponding to the irreducible representation A_{1g} mediate the cooperative interaction between the magnetic moments, giving rise to an orbitally ordered state.

PACS number(s): 75.30.Gw, 75.40.Cx, 78.70.Dm

I. INTRODUCTION

Like their cubic counterparts, hexagonal perovskites have the general composition $AB\text{O}_3$ and can be described as a close packing of $A\text{O}_3$ layers wherein the B cations occupy 1/4 of the octahedral vacancies. While the family of cubic perovskites originates from a cubic close packing of such layers (stacking sequence $abcabc\dots$), the hexagonal perovskites consist of a hexagonal close packing ($ababab\dots$). This change in the stacking sequence results in pronounced differences between the two families of perovskites. The cubic perovskites form a three-dimensional network of corner-sharing $B\text{O}_6$ octahedra with rather long metal-metal distances of 3.8 Å and B-O-B angles identical to (or at least close to) 180°. On the other hand, the aristotype of the hexagonal perovskites (the so-called $2H$ structure) consists of infinite chains of face-sharing $B\text{O}_6$ octahedra running along the c axis of the unit cell. A great number of modified structures exist, in which these $B\text{O}_6$ chains are interrupted by other building units like, for example, trigonal prisms.

One highly interesting family of such modified hexagonal perovskites possesses the general stoichiometry $[A'_2\text{O}_{1+\delta}] \times [A_n B_{n-1}\text{O}_{3n}]$. In these oxides, chains of $n-1$ face-sharing $B\text{O}_6$ octahedra are separated by an $[A'_2\text{O}_{1+\delta}]$ layer, which consists of A' cations in a trigonal prismatic coordination. The composition $A_4 B\text{O}_{7+\delta}$ ($[A'_2\text{O}_{1+\delta}][A_2 B\text{O}_6]$, i.e., $n=2$) represents an end member of this series with isolated $B\text{O}_6$ units, while the $2H$ structure can be considered the $n=\infty$ end member.

Surprisingly few examples for this family of perovskites are known so far. To the best of our knowledge, the first oxide described in literature was $\text{Ba}_5\text{Ru}_2\text{O}_{10}$,[1] which corresponds to an $n=3$ member. It was later found that in this compound an isoelectronic replacement of one oxide ion (O^{2-}) by a peroxide unit (O_2^{2-}) was possible, and the obtained sample was thus denoted as $\text{Ba}_5\text{Ru}_2\text{O}_9(\text{O}_2)$.[2] The isostructural compound $\text{Ba}_5\text{Nb}_2\text{O}_9(\text{O}_2)$ was discovered two

years later.[3] The only $n=3$ member containing a $5d$ transition metal is $\text{Ba}_{3.44}\text{K}_{1.56}\text{Ir}_2\text{O}_{10}$,[4] while the sole $n=6$ oxide known to date is $\text{La}_4\text{Ba}_{2.6}\text{Ca}_{1.4}(\text{Mn}_4\text{Ca})\text{O}_{19}$.[5] In 2000, the existence of $\text{La}_2\text{Ca}_2\text{MnO}_7$was reported.[6] This compound was the first $n=2$ member of this series. The corresponding peroxide $\text{La}_2\text{Ca}_2\text{MnO}_6(\text{O}_2)$ was later prepared by high-pressure synthesis.[7]

In 2004, our group reported on single crystals of $\text{La}_{1.2}\text{Sr}_{2.4}\text{RuO}_7$, the first $n=2$ compound to contain a $4d$ transition metal.[8] X-ray diffraction revealed a significant structural distortion within the $[A'_2\text{O}_{1+\delta}]$ layers with cations occupying an off-center position within the trigonal prisms and parts of the cationic sites remaining vacant. X-ray absorption near-edge structure (XANES) and magnetic measurements proved ruthenium to be pentavalent. A representation of the $[A'_2\text{O}_{1+\delta}][A_2 B\text{O}_6]$ structure is shown in Fig. 1.

Attempts to prepare polycrystalline material resulted in an isostructural compound with a higher strontium and oxygen content.[9] Neutron diffraction and thermogravimetric measurements revealed the presence of peroxide ions leading to the composition $\text{La}_{1.2}\text{Sr}_{2.7}\text{RuO}_{6.67}(\text{O}_2)_{0.33}$.[10] It is noteworthy that all $[A'_2\text{O}_{1+\delta}][A_n B_{n-1}\text{O}_{3n}]$ oxides described earlier contain either oxide or peroxide ions in the hexagonal voids of the $[A'_2\text{O}_{1+\delta}]$ intergrowth layer, while $\text{La}_{1.2}\text{Sr}_{2.7}\text{RuO}_{6.67}(\text{O}_2)_{0.33}$ represents an intermediate composition with both O^{2-} and O_2^{2-} ions being simultaneously present.

In a systematic study to replace ruthenium by other platinum group metals, we furthermore discovered $\text{La}_{1.2}\text{Sr}_{2.7}\text{IrO}_{6.67}(\text{O}_2)_{0.33}$.[10] This iridate was found to be isostructural to the corresponding ruthenate and showed a small temperature-independent paramagnetism, which could conclusively be explained taking into account the strong spin-orbit coupling of the $^3T_{1g}$ ground term of the Ir^{5+} ions. Almost simultaneously with our work, Mugavero, Smith, and zur Loye reported on $\text{La}_{2.5}\text{K}_{1.5}\text{IrO}_7$.[11] These two compounds are hitherto the only $n=2$ members of the $[A'_2\text{O}_{1+\delta}] \times [A_n B_{n-1}\text{O}_{3n}]$ series of hexagonal perovskites containing a $5d$ transition metal.
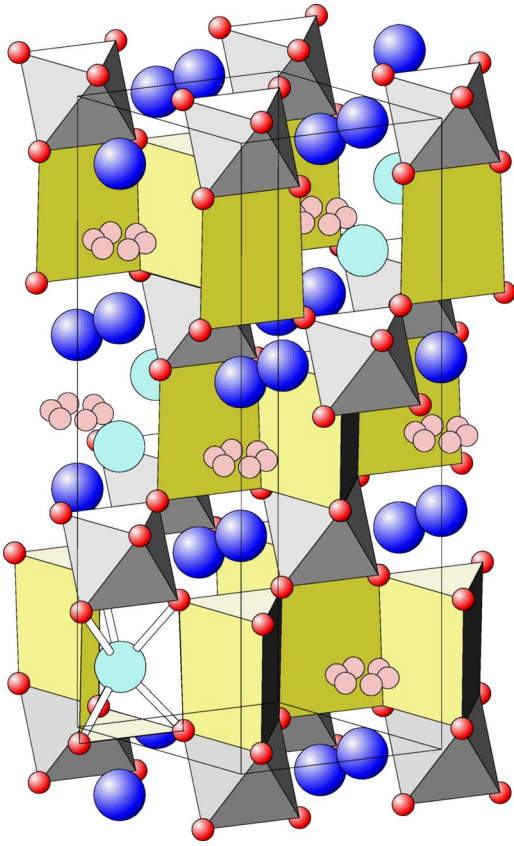
FIG. 1. (Color online) Crystal structure of the $[A_2'O_{1+\delta}]$ $\times[A_2BO_6]$-type hexagonal perovskites. A' cations in the trigonal prisms and A cations in the A_2BO_6 layers are shown as large unshaded spheres and shaded spheres, respectively. Oxygen ions in the $[A_2'O_{1+\delta}]$ layers are represented by small unshaded spheres.

Both $La_{1.2}Sr_{2.7}RuO_{7.33}$ and $La_{1.2}Sr_{2.7}IrO_{7.33}$ have very low electrical conductivities. Recent studies on their dielectric behavior revealed a variable-range hopping mechanism for the electrical transport and relaxation processes due to ionic displacements.[12]

During our investigations of magnetic properties, we found a strong magnetic frustration in $La_{1.2}Sr_{2.7}RuO_{6.67}(O_2)_{0.33}$, which very likely originates from the geometric arrangement of the paramagnetic centres. Geometrically frustrated oxides are an interesting class of magnetic systems, and this type of frustration has only been observed for a small number of magnetic lattices,[13] having either a two-dimensional (2D) character like in the triangular or in the kagomé lattice or being three dimensional as, for example, in the pyrochlore $Dy_2Ti_2O_7$. As described in this paper, the arrangement of paramagnetic ions in the $[A_2'O_{1+\delta}][A_2BO_6]$-type hexagonal perovskites represents a new example for a geometrically frustrated lattice type, in which the frustration can in principle be of both 2D and 3D character.

II. EXPERIMENTAL DETAILS

Polycrystalline samples were prepared by conventional solid-state reaction in air for 36 h at 1250°C. Starting mate-

rials were $SrCO_3$ and predried La_2O_3 and RuO_2. A structure analysis of the basis of joint Rietveld refinements of x-ray and neutron diffraction patterns recorded at room temperature is described in detail in Ref. 10. The determined oxygen content of 7.33 for the polycrystalline ruthenate was additionally verified by thermogravimetry.

Crystals were grown by the floating zone technique. The applied growth furnace (model GERO SPO) is equipped with two 1000-W halogen lamps, the radiation of which is focused by gold-coated ellipsoidal mirrors. Polycrystalline bars serving as seed and feed rods were cold pressed and sintered in air for 10 h at 1050°C. It was found necessary to add a small excess of 10 mol % RuO_2 to the material of the feed rod to account for the evaporation of ruthenium oxide at the very high temperatures required for the melting process. Crystal growth was performed in synthetic air (0.2 l/min) at a pressure of 4 bars using a quartz flow tube of optical quality. The seed rod was rotated with a speed of 30 rpm, while the feed was kept still.

X-ray absorption spectroscopy at the Ru K edge was carried out at the beamline X1 of the Hamburger Synchrotronstrahlungslabor (HASYLAB) at the Deutsches Elektronensynchrotron (DESY). A powder from a well-ground piece of the crystal was mixed with polyethylene and pressed to a thin pellet of 13 mm diameter. XAS measurements were performed in transmission mode with a step width of 0.5 eV and a counting time of 2 s per data point. The energy was calibrated against the spectrum of Ru metal, which was measured simultaneously.

Magnetic measurements in the temperature range 1.8 $<T<300$ K were done using a Quantum Design MPMS7 superconducting quantum interference device (SQUID) magnetometer. Both zero-field-cooled (ZFC) and field-cooled (FC) data were recorded in external fields of 0.1 and 2 T, respectively. The obtained values were corrected for the diamagnetic moment of the empty sample holder.

The temperature-dependent heat capacity was investigated by means of a quasiadiabatic step heating technique with a Quantum Design PPMS system. The measurements were done on a 14-mg crystal thermally connected by grease (Apiezon N) at temperatures ranging from 1.8 K up to 300 K. The general concept and reliability of heat-capacity measurements using the PPMS instrument is reported by Lashley *et al.*[14] The uncertainty of the measurements reported in this paper is estimated to be below 2%.

Neutron diffraction at $T=1.5$ K was carried out on the HRPT diffractometer at PSI, Villigen (Switzerland) using the following experimental conditions: $\lambda=1.494$ Å, 2θ range $5°-165°$, 2θ step size 0.05°. For Rietveld refinements the FULLPROF program suite was used.[15]

III. RESULTS AND DISCUSSION

Magnetic measurements performed on polycrystalline $La_{1.2}Sr_{2.7}RuO_{7.33}$ revealed a sharp cusp in the dc susceptibility ($\chi=m/B$) at 7 K (Fig. 2). A Curie-Weiss fit of the reciprocal susceptibility in the region above 50 K leads to a magnetic moment of $3.97\mu_B$ per ruthenium ion, in good agreement with the spin-only value of $3.87\mu_B$ expected for
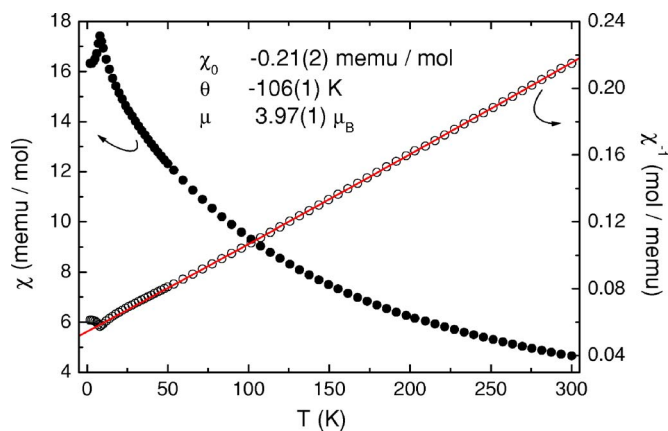
FIG. 2. (Color online) χ_{mol} of polycrystalline $La_{1.2}Sr_{2.7}RuO_{7.33}$ as a function of temperature (left scale) and inverse susceptibility (right scale) including the fit by a Curie-Weiss law (solid line).

the $^4A_2$ ground state of Ru^{5+} ions.[9] The Weiss constant was determined to be -106 K, a value 15 times larger than the ordering temperature T_N. A ratio $|\theta|/T_N$ significantly larger than 10 is usually considered an indication for a frustrated magnetic system, and this ratio is therefore frequently denoted as frustration index.[16] Magnetic frustration occurs when a large fraction of magnetic moments is subject to competing, antagonistic couplings. In these cases it is not possible to satisfy all individual interactions simultaneously; i.e., parts of the magnetic moments have an unfavorable mutual alignment, whatever orientation they take. This magnetic frustration often arises from the specific geometric arrangement of antiferromagnetically interacting paramagnetic ions—for example, in a triangular array or in the so-called kagomé lattice.[17]

The magnetic frustration in $[A_2'O_{1+\delta}][A_2BO_6]$-type perovskites probably also originates from the geometric arrangement of the paramagnetic transition metal ions. To understand how such a geometric magnetic frustration can arise in $La_{1.2}Sr_{2.7}RuO_{7.33}$ it is useful to plot the structure in a highly simplified manner. Figure 3 shows in the left part the classical structure drawing in comparison to a representation consisting of ruthenium polyhedra. As can be seen, the rhom-

bohedral lattice can be considered as an arrangement of (elongated) edge-sharing Ru_4 tetrahedra. In these tetrahedra two possibilities for geometric magnetic frustration exist: on the one hand, the basal plane (the crystallographic ab plane) forms a triangular lattice. As schematically illustrated in the right part of Fig. 3, only two out of three spins in each triangle can align according to their antiferromagnetic interaction, while the third one is frustrated. Considering the entire tetrahedra, on the other hand, only two out of four spins of each tetrahedron can take an antiparallel orientation, while the remaining two are frustrated. Such a geometric magnetic frustration is, for example, found in the fcc lattice. The $R\bar{3}m$ lattice can indeed be considered a link between the 3D-frustrated fcc and the 2D-frustrated triangular lattice: For undistorted Ru_4 tetrahedra the arrangement of paramagnetic ions is the same as in the fcc lattice while for a very strong (i.e., infinite) elongation of the tetrahedra the triangular lattice results. Since the distances between neighboring ruthenium ions in the basal plane and from this plane to an ion at the tip of an elongated tetrahedron are quite similar in $La_{1.2}Sr_{2.7}RuO_{7.33}$ (roughly 5.8 Å and 6.9 Å, respectively), it is to assume that the interactions between these different types of neighbors might be of the same order of magnitude. Therefore the magnetic frustration may either be restricted to the basal plane or include the entire tetrahedra.

To gain a deeper insight into the origin of the frustration, it was necessary to measure the angular-dependent magnetic properties; i.e., the magnetic response parallel and perpendicular to the crystallographic c axis had to be examined. Since crystals earlier obtained from a $BaCl_2$ flux[8] were by far too small for such measurements, a number of attempts were made to grow single crystals by optical floating zone melting. The best results were obtained from an experiment under 4 bars of synthetic air and with a 10 mol % excess of RuO_2 in the feed rod. From the obtained boule different single crystals were isolated, the largest of which was approximately $3 \times 2 \times 2$ mm^3 in size. This crystal was used for the angular-dependent measurements described in the following. The crystal could easily be oriented since it cleaved perpendicular to the c axis. Laue backscattering diffraction was used to confirm the correct orientation. Electron probe microanalysis (EPMA) yielded the composition
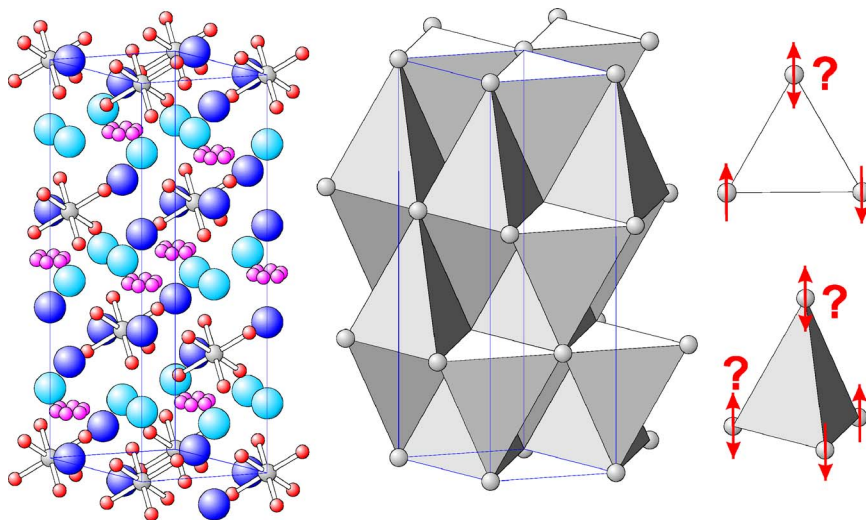

FIG. 3. (Color online) Crystal structure of $(La,Sr)_{4-z}RuO_{7+\delta}$ as classical *ball and stick* representation (left) and shown as arrangement of elongated Ru_4 tetrahedra (middle). The right part of the figure demonstrates two possibilities of geometric magnetic frustration in this arrangement.
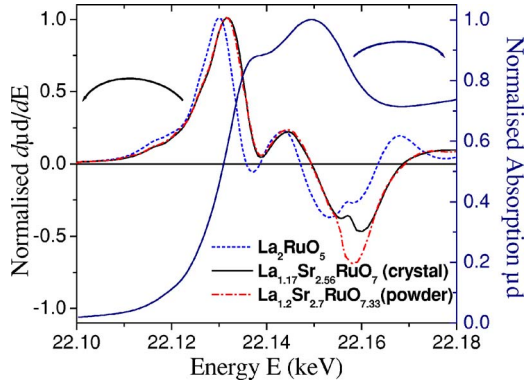
FIG. 4. (Color online) Normalized absorption (right scale) and first derivative of the absorption spectrum (left scale) of the floating-zone-grown crystal. Dashed and dash-dotted lines correspond to reference samples containing Ru^{4+} and Ru^{5+}, respectively.

FIG. 5. (Color online) Anisotropy of the magnetic susceptibility of $(La,Sr)_{4-z}RuO_{7+\delta}$. (a) low-temperature region of χ. (b) $1/\chi$ plotted for the entire measured temperature range. A minor diamagnetic contribution was subtracted for clarity.

$La_{1.17(1)}Sr_{2.56(2)}RuO_{6.82(4)}$. The numbers in brackets are the estimated standard deviations from 50 measuring points across the crystal surface. It should be noted that the lanthanum content is close to its expected value, whereas the strontium content is slightly smaller. The total composition is similar to the one of the flux-grown single crystals described in Ref. 8 ($La_{1.2}Sr_{2.4}RuO_7$) and manifests a cationic deficiency, which is typical for this class of hexagonal perovskites. Powder x-ray diffraction was performed on a ground piece of crystal to verify the phase purity. The obtained cell parameters of $a=5.761(1)$ Å and $c=18.244(3)$ Å agree well with the values found for the crystals grown from $BaCl_2$ flux ($a=5.760$ Å, $c=18.273$ Å) in accordance with the very similar composition. It is furthermore apparent that the floating-zone-grown crystals do not contain peroxide ions, again in accordance with those crystals obtained by flux growth.

Apart from their compositional deviations, single crystals and polycrystalline samples showed remarkably similar physical properties as discussed below. For this reason, a more generalized composition $(La,Sr)_{4-z}RuO_{7+\delta}$ will be used in the following to embrace both single-crystalline and polycrystalline samples.

To verify the oxidation state of ruthenium in the grown crystals, x-ray absorption spectroscopy was applied. In a series of recently published papers, we showed the usefulness of XANES investigations at the Ru L_{III} threshold (≈ 2.84 keV) for this purpose.[8–10,18,19] Here, we demonstrate that also measurements at the Ru K edge (≈ 22.12 keV) may be used, despite the by far lower resolution at these high energies. Figure 4 depicts the Ru K-edge XANES region of a powdered piece of the floating-zone-grown crystal and the first derivative of the spectrum in comparison to two reference oxides containing Ru^{4+} and Ru^{5+}, respectively. As can be seen, the absorption spectrum closely resembles the one of the Ru^{5+} reference, for which the polycrystalline $La_{1.2}Sr_{2.7}RuO_{6.67}(O_2)_{0.33}$ was chosen. The presence of Ru^{5+} in this sample has been established using various different reference oxides as described in more detail in Ref. 9. In contrast, the absorption features of the Ru^{4+}-containing reference La_2RuO_5 are located at a considerably lower energy. This shift of the absorption edge towards higher energies
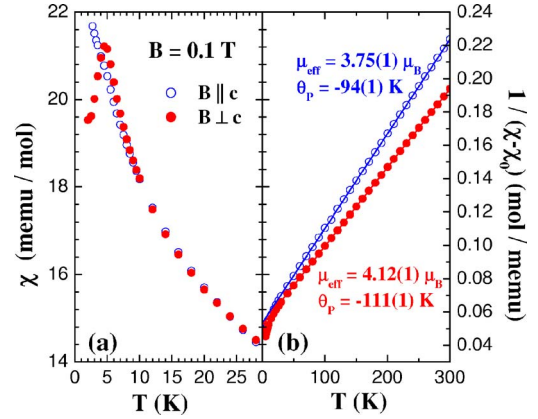
with increasing oxidation number is known as the so-called "valence shift." It results from the fact that the positive electric charge of the nucleus is partially shielded by the d electrons. An oxidation of the metal reduces the number of valence electrons. Consequently, the effective core charge increases and the inner electrons become more tightly bound, leading to a shift of the absorption edge towards higher energies.

For the determination of the valence state of ruthenium in perovskites, the second derivatives have repeatedly been used.[20,21] At least for our spectra, this procedure required a considerable smoothing of the data, which may introduce bias in the results. On the other hand, some features of the absorption spectra are not well resolved if the original data are used. We therefore chose the first derivatives as a compromise. As can be seen in Fig. 4 the most pronounced features of the derivative spectra are a maximum at approximately 22.131 keV and a zero crossing at 22.149 keV. Going from Ru^{4+} to Ru^{5+} these signatures a shift by 1.7 eV and 2.5 eV to higher energies. The values are consistent with results found in the literature[20] and prove the presence of pentavalent ruthenium in the floating-zone-grown crystals.

Magnetic measurements of the above-described crystal with the external field parallel to the c axis and within the ab plane, respectively, are shown in Fig. 5. An anisotropy of the magnetic moment is evident. While for $\mathbf{B}\|c$ an n_{eff} value of 3.75(1) was found, the corresponding value for $\mathbf{B}\perp c$ was determined to be 4.12(1) ($n_{eff}=\mu/\mu_B$ is the number of effective Bohr magnetons). The root mean square $\left[\sqrt{\frac{1}{3}(n_{eff\|})^2+\frac{2}{3}(n_{eff\perp})^2}\right]$ is equal to 4.00(1). This value agrees well with the one of 3.97 found for the polycrystalline material and is close to the expected result of 3.87, the deviation being only 3.3%.

The difference in $n_{eff\|}$ and $n_{eff\perp}$ is surprising, since for a pure S state resulting from the $^4A_2$ ground term of Ru^{5+} an isotropic magnetic behavior is expected. One possible explanation is a slight deviation from the ideal O_h symmetry—for example, due to a stretching or compression of the RuO_6 octahedra parallel to the c axis.

To investigate the crystal structure below the magnetic transition, a powder neutron diffraction pattern was recorded

TABLE I. Structural parameters of $La_{1.2}Sr_{2.7}RuO_{7.33}$ at 1.5 K derived from powder neutron diffraction. Space group $R\bar{3}m$ (166), $a=5.7420(5)$, $c=18.311(1)$, $R_p=2.89$, $R_{wp}=3.79$, and $\chi^2=4.51$.

Atom	Site	Occupation	x	y	z	B_{iso} (Å^2)
Ru	3a	1	0	0	0	0.74(2)
O(1)	18h	1	0.3174(2)	0.1587(2)	0.06103(5)	3.70[a]
La(1)/Sr(1)	6c	0.6/0.4	0	0	0.62334(4)	0.73(2)
Sr(2)	6c	0.764(7)	0	0	0.17499(6)	0.50(4)
Sr(2a)	18h	0.064(2)	0.130(2)	0.065(2)	0.17895(46)	0.50(4)
O(2)	18g	0.042(3)	0.168(4)	0	0.5	0.37(8)
O(2a)	18h	0.183(3)	0.1424(7)	0.0712(7)	0.5	0.37(8)

[a]Refined with the following anisotropic displacement parameters: $\beta_{11}=2\beta_{12}=0.0043(3)$, $\beta_{22}=0.0698(5)$, $\beta_{33}=0.00119(3)$, $\beta_{12}=0.0021(3)$, $\beta_{13}=2\beta_{23}=-0.00044(9)$.

at $T=1.5$ K. Starting from the structural model described in Ref. 10, a good agreement in the Rietveld calculations was achieved. The corresponding results are listed in Table I. No indications for a structural phase transition were found. Upon cooling both cell parameters a and c shrink by 0.2%. The Ru-O distance of 1.934(1) Å at 1.5 K is almost identical to the value found at room temperature [1.932(2) Å]. The O(1)-Ru-O(1) bond angles are 90.05(8)°, indicating an undistorted octahedral coordination geometry.

Although the RuO_6 units apparently possess perfect O_h symmetry, the presence of the other ions (for example, the next ruthenium neighbors) reduces the local point symmetry to $\bar{3}m$ (D_{3d}) as discussed below. Fluctuations in the occupation of the La(1)/Sr(1) site or of the partially occupied Sr(2) and Sr(2a) sites (see Table I) may further reduce the symmetry of the Ru ions, resulting in an anisotropic magnetic behavior. Since the crystal field cannot directly interact with the spin, the anisotropy of χ indicates that the angular momentum is not completely quenched, most likely because of the admixture of higher-order terms to the $^4A_2$ ground term.

Looking at Fig. 5 two additional peculiarities become evident. First, for both $\mathbf{B}\|c$ and $\mathbf{B}\perp c$ the Weiss constant is large and negative, indicating a strong antiferromagnetic interaction between the magnetic moments. Within the ab plane the absolute value is about 15% larger, revealing that the corresponding spin-spin interaction is stronger. This observation is in agreement with the shorter Ru-Ru distance within this plane. Again, the root mean square of $\theta_\|$ and $\theta_\perp$ of −106 K is in very good accordance with the Weiss constant of −106 K for the polycrystalline sample. The second striking result is that only for $\mathbf{B}\perp c$ is a clear cusp in the susceptibility data found. Its temperature of $T_N\approx 5$ K is slightly smaller than the 7 K found for the polycrystalline material. Since, on the other hand, $|\theta|$ is larger (−111 K vs −106 K), a frustration index of roughly 25 is obtained, in contrast to the value of 15 for the polycrystals. For the magnetic field applied parallel to the crystallographic main axis, no such clear cusp can be found. The minor change in the slope visible in Fig. 5(a) is very likely caused by a minimal misalignment of the crystal in the SQUID magnetometer.

From these results it can be concluded that for $(La,Sr)_{4-z}RuO_{7+\delta}$ a (highly frustrated) magnetic ordering exists only within the triangular lattice of the ab planes, while

parallel to the c axis no such ordering of the magnetic moments occurs down to 1.8 K. The low-temperature neutron diffraction results support this interpretation: Although the Rietveld refinement led to a very good agreement of measured and calculated patterns, some small low-angle peaks in the 1.5 K diffraction pattern could not be refined. The most pronounced peak at $2\theta\approx 9.9°$ is shown in Fig. 6. Several hints indicate that the additional low-temperature peaks are not due to structural changes but originate from a magnetic ordering. First, they can only be observed at very low diffraction angles. This points to a magnetic origin, because unlike the nuclear scattering lengths the magnetic form factors strongly decrease with increasing θ. Second, these peaks are much broader than the nuclear reflections, which indicates a very low "grain size" of the magnetic domains, in accordance with the proposed frustration. Finally, for the isostructural compound $La_{1.2}Sr_{2.7}IrO_{7.33}$, which does not show any magnetic ordering,[10] no corresponding peaks were detected at 1.5 K. The peak at $2\theta\approx 9.9°$ can be indexed if the a axis of the unit cell is doubled. This supports the scenario of a formation of an ordered state within the ab plane as deduced from the susceptibility data. No attempts were made,
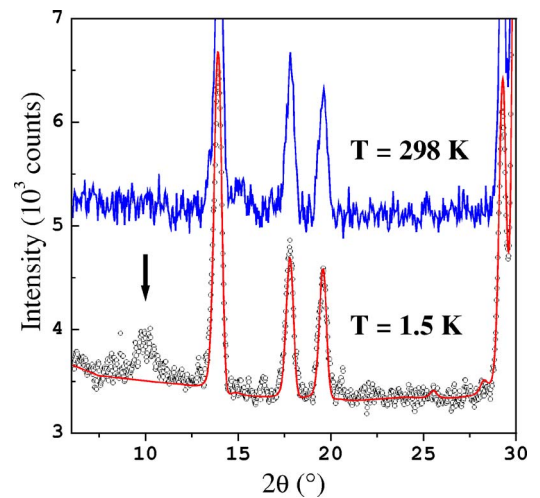

FIG. 6. (Color online) Low-angle region of the Rietveld ND refinement of $La_{1.2}Sr_{2.7}RuO_{7.33}$ at 1.5 K. One additional magnetic peak is marked by an arrow. The room-temperature diffraction pattern is shown for comparison.
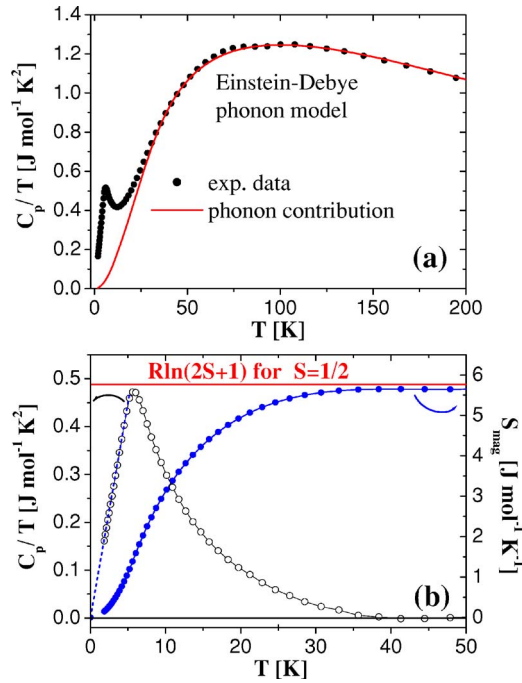
FIG. 7. (Color online) (a) Specific heat of $(La,Sr)_{4-z}RuO_{7+\delta}$ and fit of the lattice contribution. (b) Magnetic part of C_p/T (left scale) and resulting magnetic entropy (right scale). The horizontal line represents the expected value for $S=1/2$.

though, to refine the magnetic structure because the respective peaks were too small and broad.

In many cases magnetic frustration gives rise to a spin-glass behavior, indicated, for example, by pronounced differences between the FC and ZFC magnetization below the glass transition temperature (T_f). With an increase of the external magnetic field, T_f shifts to lower temperatures. Furthermore, ac susceptibility measurements of spin glasses exhibit a sharp maximum in the real part (χ') of the susceptibility at T_f. This maximum becomes broader with both increasing frequency and magnetic field and is accompanied by a point of inflection in the imaginary part (χ'') of the susceptibility.

To investigate a possible spin-glass magnetization in $(La,Sr)_{4-z}RuO_{7+\delta}$, frequency- and field-dependent measurements were carried out. No significant differences between the FC and ZFC magnetization were detected for polycrystalline samples and the floating-zone-grown crystal. The temperature of the cusp in the dc susceptibility did not show any dependence on the external field of 0.1 and 2 T, respectively. Finally, ac susceptibility measurements (not shown) yielded identical χ' values in the frequency range from 1 Hz to 1 kHz, while χ'' was extremely weak and constant for all frequencies. From these investigations, we can rule out a spin-glass-type magnetism for $(La,Sr)_{4-z}RuO_{7+\delta}$.

Specific heat measurements were performed to further investigate the magnetic ordering. Figure 7(a) shows the C_p/T data of the same crystal as used for magnetic investigations. A clear peak at 5.5 K indicates a pronounced magnetic contribution to the heat capacity.

In order to separate electronic and lattice contributions the latter were calculated using one Debye term and three Einstein modes. As starting parameters for the Einstein temperatures, values derived by infrared spectroscopy were used.[12] The number of internal degrees of freedom was fixed to 36, according to the 12 atoms in the unit cell. Using a weight distribution $3:9:12:12$, a Debye temperature of $\Theta_D=116$ K, and three Einstein temperatures of $\Theta_{E1}=173$ K, $\Theta_{E2}=362$ K, and $\Theta_{E3}=665$ K were obtained. The solid red line in Fig. 7(a) shows the corresponding fit.

Subtraction of this fit as lattice contribution leads to the magnetic C_p/T values depicted in Fig. 7(b). Apparently, there is a linear behavior of $C_{p(magn)}/T$ below T_N, which allows us to extrapolate the measurements down to $T=0$ K. In general, for a magnet possessing long-range ordering C_p is proportional to $T^{d/\nu}$, where d is the dimensionality (2 in the case of two-dimensional) and ν reflects the exponent in the excitation dispersion (1 for antiferromagnets). Therefore, the linear dependence of C_p/T on T is consistent with a (frustrated) antiferromagnetic ordering in two dimensions and confirms our magnetic measurements.

Similar linear relationships of $C_p/T \sim T$ below the ordering temperature have also been described for other geometrically frustrated systems like the triangular $SrCr_8Ga_4O_{19}$, the kagomé-lattice compound $KCr_3(OH)_6(SO_4)_2$, and in the delafossite structure material $Gd_{0.8}La_{0.2}CuO_2$.[16] In these systems, the magnetic lattices are of two-dimensional character. This similarity is another support for the observed 2D order in $(La,Sr)_{4-z}RuO_{7+\delta}$.

As can be seen in Fig. 7(b), $C_{p(magn)}/T$ reaches zero at roughly 40 K. This is in agreement with the magnetic measurements shown in Figs. 2 and 5(b), which reveal a Curie-Weiss behavior (i.e., the complete breakdown of magnetic ordering) at this temperature.

Integration of $C_{p(magn)}/T$ leads to the magnetic entropy according to

$$\int \frac{C_{p(magn)}}{T} dT = S_{(magn)} = R \ln(2S+1).$$

Here $S_{(magn)}$ and S refer to the magnetic entropy and the spin, respectively. The corresponding graph is shown on the right scale of Fig. 7(b). Obviously, the experimentally found magnetic entropy is much smaller than expected for an $S=3/2$ system. To examine the influence of our model on the lattice contribution, we performed several fits using different starting parameters and weighting schemes. For all runs, $S_{(magn)}$ was found to be 5.6 J mol^{-1} K^{-1} within a range of $\pm15\%$. This value can be explained either by $S_{(magn)}=\frac{1}{2}R\ln\left(2\times\frac{3}{2}+1\right)$ or by $S_{(magn)}=R\ln\left(2\times\frac{1}{2}+1\right)$. The former equation corresponds to a situation in which the full spin of every second Ru ions takes part in the magnetic ordering while the latter equation describes a magnetic ordering of all Ru ions, each contributing a reduced spin of $S=1/2$. From the geometric arrangement of the paramagnetic ions we do not find any reason for only half of the ions to magnetically order. On the contrary, since all Ru ions are symmetry equivalent, they are expected to show the same magnetic behavior.

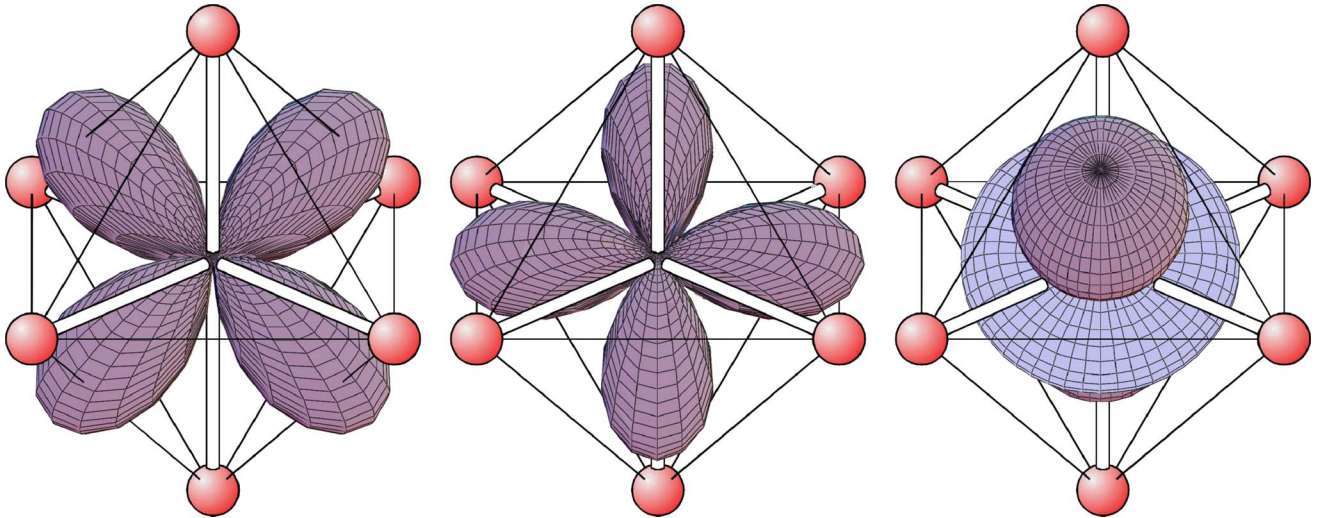On the other hand, a frustrated magnetic ordering corresponding to a spin $S=1/2$ and being restricted to the *ab*

FIG. 8. (Color online) RuO_6 octahedron in $(La,Sr)_{4-z}RuO_{7+\delta}$ viewed nearly along c with the symmetry-adapted t_{2g} orbitals superimposed. From left to right: $d_{x'y'}$, $d_{x'^2-y'^2}$ (E_g) and $d_{z'}^2$ (A_{1g}). Only the "belt" of the $d_{z'}^2$ orbital enables a collective magnetic coupling.

plane can be explained on the basis of symmetry considerations. While the RuO_6 units form ideal octahedra, the presence of the surrounding ions (especially the Ru neighbors) reduces the local symmetry to $\bar{3}m(D_{3d})$. In this point group, the three t_{2g} orbitals of the octahedral point group O_h split into two sets, which transform according to the irreducible representations $A_{1g}(d_{z'}^2)$ and $E_g(d_{x'y'}, d_{x'^2-y'^2})$. Figure 8 illustrates the corresponding wave functions superimposed to a RuO_6 octahedron. In this context, it is important to emphasize that the $d_{z'}^2$ and $d_{x'^2-y'^2}$ orbitals are *not* identical to the e_g orbitals usually shown for octahedral crystals fields. These two orbitals still belong to the t_{2g} set but are symmetry-adapted linear combinations of these states. The identical names result from a different choice of coordinate system: while in O_h one fourfold symmetry axis is taken as z, in D_{3d}, z' corresponds to the threefold axis. A prime is therefore used to identify this different coordinate system. From Fig. 8 it can be seen that only the $d_{z'}^2$ orbitals have the appropriate symmetry to interact with all nearest ruthenium neighbors within the ab plane simultaneously. For this reason, only the one electron occupying this orbital is involved in the ordering and, as a consequence, the magnetic entropy corresponds to a spin of only $1/2$. The magnetic interaction thus breaks the degeneracy of the three t_{2g} orbitals, resulting in an orbitally ordered state.

IV. CONCLUSIONS

The hexagonal perovskite $(La,Sr)_{4-z}RuO_{7+\delta}$ is a new example of a geometrically frustrated magnetic system. Its magnetic sublattice consists of edge-sharing elongated tetrahedra, which form a triangular arrangement parallel to the crystallographic ab direction. Crystals of several mm size

were successfully grown by the floating zone technique. Magnetic measurements in an external field parallel and perpendicular to the c direction revealed a frustrated magnetic ordering only within the ab plane, although comparable Weiss constants for $\mathbf{B} \| c$ and $\mathbf{B} \perp c$ indicate a similar strength of the magnetic interactions in the different directions. A frequency-dependent investigation of the ac susceptibility led to identical magnetic responses regardless of the measurement conditions. A spin-glass magnetization behavior can therefore be ruled out.

Studies of the heat capacity showed a linear dependence of $C_{p(magn)}/T$ vs T below the transition temperature as already observed for other frustrated antiferromagnetic 2D lattices. The magnetic contribution to the entropy shows that only a reduced spin of $S=1/2$ participates in the magnetic ordering. From symmetry considerations we conclude that only one of the t_{2g} orbitals possesses a compatible orientation to allow for a collective interaction and, consequently, only the one electron occupying this orbital takes part in the magnetic ordering. For this reason, the antiferromagnetic transition is correlated to an orbital ordering of the t_{2g} orbitals.

*Corresponding author. FAX: ++49 821 598 3002. Electronic address: stefan.ebbinghaus@physik.uni-augsburg.de

[1] C. Dussarrat, J. Fompeyrine, and J. Darriet, Eur. J. Solid State Inorg. Chem. **31**, 289 (1994).

[2] F. Grasset, C. Dussarrat, and J. Darriet, J. Mater. Chem. **7**, 1911 (1997).

[3] F. Grasset, M. Zakhour, and J. Darriet, J. Alloys Compd. **287**, 25 (1999).

[4] S. J. Kim, M. D. Smith, J. Darriet, and H. C. zur Loye, J. Solid State Chem. **177**, 1493 (2004).

[5] L. J. Bie, Y. X. Wang, J. H. Lin, C. K. Loong, J. W. Richardson, L. P. You, and C. Dong, Chem. Mater. **15**, 516 (2003).

[6] Y. Wang, J. Lin, Y. Du, R. Qin, B. Han, and C. K. Loong, Angew. Chem., Int. Ed. **39**, 2730 (2000).

[7] E. Gaudin, G. Goglio, A. Besnard, and J. Darriet, J. Solid State Chem. **175**, 124 (2003).

[8] S. G. Ebbinghaus, J. Solid State Chem. **177**, 817 (2004).

[9] T. Götzfried, A. Reller, and S. G. Ebbinghaus, Solid State Sci. **6**, 1205 (2004).

[10] T. Götzfried, A. Reller, and S. G. Ebbinghaus, Inorg. Chem. **44**, 6550 (2005).

[11] S. J. Mugavero III, M. D. Smith, and H. C. zur Loye, J. Solid State Chem. **178**, 3176 (2005).

[12] P. Lunkenheimer, T. Götzfried, R. Fichtl, S. Weber, T. Rudolf, A. Loidl, A. Reller, and S. G. Ebbinghaus, J. Solid State Chem. **179**, 3965 (2006).

[13] A. P. Ramirez, MRS Bull. **30**, 447 (2005).

[14] J. C. Lashley, M. F. Hundley, A. Migliori, J. L. Sarrao, P. G. Pagliuso, T. W. Darling, M. Jaime, J. C. Cooley, W. L. Hults, L. Morales, D. J. Thoma, J. L. Smith, J. Boerio-Goates, B. F. Woodfield, G. R. Steward, R. A. Fisher, and N. E. Phillips, Cryogenics **43**, 369 (2003).

[15] J. Rodríguez-Carvajal (unpublished).

[16] A. P. Ramirez, Annu. Rev. Mater. Sci. **24**, 453 (1994).

[17] J. E. Greedan, J. Mater. Chem. **11**, 37 (2001).

[18] S. Ebbinghaus, Z. Hu, and A. Reller, J. Solid State Chem. **156**, 194 (2001).

[19] Z. Hu, H. von Lips, M. S. Golden, J. Fink, G. Kaindl, F. M. F. de Groot, S. Ebbinghaus, and A. Reller, Phys. Rev. B **61**, 5262 (2000).

[20] J.-H. Choy, S.-H. Hwang, G. Demazeau, and D.-Y. Jung, J. Phys. IV **7**, C2-764 (1997).

[21] J.-H. Choy, J.-Y. Kim, S.-H. Hwang, S.-J. Kim, and G. Demazeau, Int. J. Inorg. Mater. **2**, 61 (2000).